THE ASTROPHYSICAL JOURNAL, 253:975–982, 1982 February 15

RELATIONSHIPS BETWEEN THE ENERGETICS OF IMPULSIVE AND GRADUAL EMISSIONS FROM SOLAR FLARES

CAROL JO CRANNELL, JUDITH T. KARPEN,[1] AND ROGER J. THOMAS
Laboratory for Astronomy and Solar Physics, Goddard Space Flight Center
Received 1981 March 9; accepted 1981 August 21

ABSTRACT

The gradual soft X-ray emissions associated with a homogeneous set of solar flares have been investigated in the context of a thermal model proposed to explain the impulsive components. The parametric techniques which successfully characterized the hard X-ray and microwave observations are employed in an event-by-event analysis to test for quantitative and correlative relationships between the impulsive and gradual emissions. The results of this investigation are consistent with the hypothesis that the hard X-ray and microwave emissions are produced by bulk heating of a common thermal source. The quantitative relationships require an additional source to explain the soft X-ray observations, consistent with previous results. Correlations between the energetics of the impulsive and gradual emissions, identified in the present work, provide the first clear evidence that their energizing mechanisms are related.

Subject headings: radiation mechanisms — Sun: flares — Sun: radio radiation — Sun: X-rays

I. INTRODUCTION

The time-intensity profiles of hard X-ray and microwave emissions from solar flares exhibit a wide variety of temporal complexity. From a study of solar hard X-ray bursts, van Beek, de Feiter, and de Jager (1974) suggested that the observed emissions may be comprised of a cluster of simple spikes, denoted "Elementary Flare Bursts" (EFBs). This concept was tested in subsequent studies, in which it was found that flares selected from the *TD 1* A hard X-ray data could be decomposed completely into EFBs. The validity of the concept was corroborated further by the observation that, within each flare, the time-intensity profiles of EFBs were homologous (van Beek, de Feiter, and de Jager 1976; de Jager and de Jonge 1978). Similar results were obtained for independent microwave observations of solar flares by Wiehl (1976) and Kauffman and Iacomo (1977).

To better understand the dynamics of impulsive solar phenomena, Crannell *et al.* (1978) investigated a set of simple impulsive spike bursts. The selection of these events was motivated by the fact that they evinced the simplest impulsive time structure of all solar flares identified in the *OSO 5* hard X-ray data. The results of this study suggested that the X-ray and microwave emission originated in a common thermal source. Further evidence for a thermal process was reported by Matzler *et al.* (1978), in a detailed analysis of the dynamic hard X-ray spectra and associated emissions for the two most intense spike bursts. In addition, Elcan (1978) has found that single temperature thermal emission gives the best fit to the hard X-ray spectra of impulsive flares observed by *OSO 7*.

The successful representation of the simple impulsive spike bursts with the hypothesis of a common, thermal plasma provides the framework for a new examination of possible relationships between impulsive and gradual emissions. The success of the EFB concept gives added impetus for investigating the variety of emissions associated with single-spike flares. An opportunity to perform such an investigation, the subject of the present work, was provided by the availability of soft X-ray observations (1 to 8 Å and 0.5 to 3 Å) for most of the original *OSO 5* spike bursts.

It would be quite satisfying (and mathematically simpler) if the entire flare associated spectrum were completely explained with a single underlying mechanism—that responsible for the impulsive emissions. It is apparent from the disparate time-intensity profiles of the hard X-ray and soft X-ray emissions, however, that some further explanation is required. The soft X-ray emission rises more slowly and is of longer duration than the associated hard X-ray emission. These characteristics, illustrated in Figure 1, are consistent with the results reported earlier for *OSO 7* observations of a larger, albeit more heterogeneous, set of events. In a study of the *OSO 7* soft X-ray bursts (5 to 15 keV), Datlowe, Hudson, and Peterson (1974) drew the following conclusion, particularly relevant to the present work: the evolution of the observed temperature and emission measure was inconsistent with the hypothesis of adiabatic compression as the direct energizing mechanism. Addition of material to the source was required to

[1]Also of the Astronomy Program, University of Maryland.

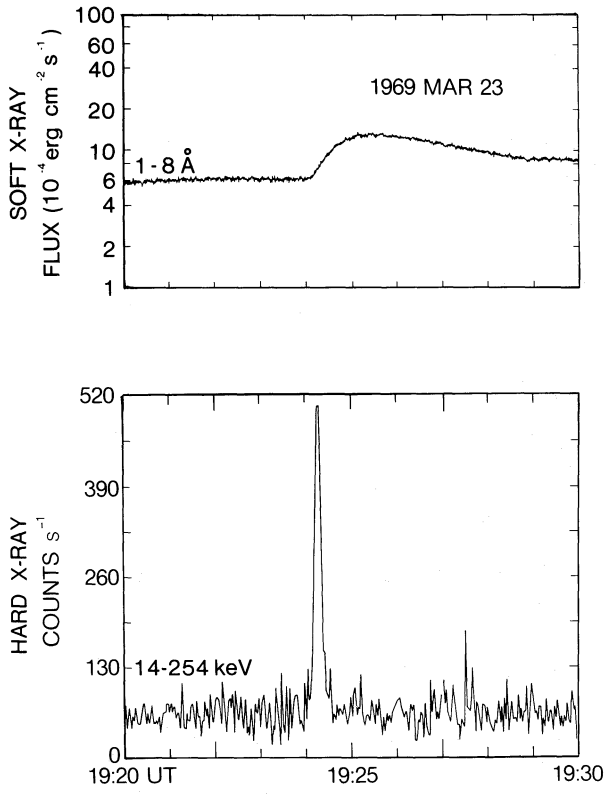

FIG. 1.—Time-intensity profiles of the observed soft X-ray and hard X-ray emissions on a common time base for one of the simple impulsive spike bursts.

describe the growth of the emission measure at the beginning of the soft X-ray burst. Datlowe, Elcan, and Hudson (1974) concluded, moreover, that heating of the soft X-ray emitting plasma was not due to the energetic electrons responsible for the associated hard X-ray bursts. This conclusion was based on the disparity of the respective time structures and on the observation that otherwise comparable soft X-ray bursts occur both with and without accompanying hard X-ray emission. While these findings rule out most direct, simple relationships, the challenge of determining the nature of the hard X-ray/soft X-ray association persists.

The approach employed in the present work uses direct confrontation, on an event-by-event basis, between the parameters characterizing the impulsive and the gradual emissions. Quantitative relationships are determined and correlations are sought to test the postulated model and to serve as guides for possible causal connections. The methods by which the required event parameters were determined are described in the next section. The analytic techniques are presented in § III, and the relationships discovered in this analysis are discussed in § IV.

II. DETERMINATION OF HARD AND SOFT X-RAY PARAMETERS

The events considered here are a set of 22 single-spike bursts identified in the *OSO 5* hard X-ray spectrometer data by Crannell *et al.* (1978). The selection criteria, the hard X-ray and microwave burst characteristics, and the techniques used to derive source properties from the hard X-ray and microwave observations are described in that reference. For the present analysis, soft X-ray observations coincident with the single-spike bursts have been obtained from the 1–8 Å ion chamber detector, flown on board the *OSO 5* satellite (Neupert 1969); and the 0.5–3 Å and 1–8 Å ion chamber detectors, flown on board the *SOLRAD 9* satellite (Kreplin and Horan 1969). Soft X-ray coverage was available for 19 of the 22 spike bursts; eight of these events were observed with both *OSO 5* and *SOLRAD 9*, six with *OSO 5* alone, and five with *SOLRAD 9* alone. The availability of data from more than one instrument, for several events, enables each instrument's coverage to be used to optimum advantage. The superior temporal resolution of the *OSO 5* ion chamber, 0.32 s, provides the best information on the time-intensity profile of the soft X-ray bursts. The *OSO 5* soft X-ray data therefore are preferred for determination of the flux levels at selected times within the events. On the other hand, the presence of two soft X-ray detectors sensitive to different wavelength bands, both on board *SOLRAD 9*, permits the derivation of effective temperatures and emission measures characterizing the soft X-ray emission.

The date, the time of hard X-ray maximum, the time of soft X-ray maximum, and the source of the soft X-ray coverage are listed in Table 1 for each event studied. For two of the 19 events, the soft X-ray observations reveal no emission associated with the hard X-ray burst. However, the *OSO 5* detector was in a low sensitivity state at these times, so that a small soft X-ray burst would not have been observable.

The parameters obtained from the hard and soft X-ray observations for use in the present analyses are defined in Table 2, together with the symbols used throughout this work to represent these parameters. The hard X-ray parameters were determined during the initial spike-burst study, and are taken from Tables 5 and 6 of Crannell *et al.* (1978). The soft X-ray parameters were obtained as described in the following paragraphs.

For *OSO 5* and for *SOLRAD 9*, the energy deposited in the 1–8 Å detectors, F_{OBS}, was calculated from the soft X-ray observations. Each of the ion chambers produced a signal in the form of a current. For the *OSO 5* detector, the ion chamber output was determined to be in one of four logarithmic ranges, from 10^{-13} to 10^{-10} A. Each range was partitioned into 256 linearly spaced intervals. The digital count rate reading, C (0–255), and the associated range, R, were recorded for each 0.32 s observing interval. The energy deposited in the *OSO 5*

TABLE 1

OBSERVED TEMPORAL PARAMETERS

Event Number	Date	Time of Hard X-Ray Maximum, UT	Time of Soft X-Ray Maximum, UT	Source of Soft X-Ray Coverage	
1	1969 Mar 1	$06^h06^m41^s.5$	$06^h07^m07^s$	*OSO 5*	*SOLRAD 9*
2	1969 Mar 1	22 53 15.1	22 54	···	*SOLRAD 9*
3	1969 Mar 8	22 07 07.1	22 08	···	*SOLRAD 9*
4	1969 Mar 18	11 55 46.4	11 56 45	*OSO 5*	*SOLRAD 9*
5	1969 Mar 22	12 11 49.9	>12 12 10	*OSO 5*	···
6	1969 Mar 23	19 24 15.5	19 25 22	*OSO 5*	···
7	1969 Mar 25	02 05 31.9	02 06 12	*OSO 5*	*SOLRAD 9*
8	1969 Mar 28	08 25 29.4	08 26 40	*OSO 5*	···
9	1969 Mar 29	07 37 45.9	[a]	*OSO 5*	···
10	1969 Mar 30	01 23 53.7	01 24 40	*OSO 5*	*SOLRAD 9*
11	1969 Jul 7	05 38 12.8	05 39 53	*OSO 5*	*SOLRAD 9*
12	1970 Mar 1	11 27 44.8	11 35	···	*SOLRAD 9*
13	1970 Jun 14	12 50 51.9	12 51 12	*OSO 5*	
14	1970 Jun 15	01 29 27.1	[b]		[b]
15	1970 Jun 15	18 38 18.2	18 41	···	*SOLRAD 9*
16	1970 Jul 5	01 37 35.4	01 38 08	*OSO 5*	*SOLRAD 9*
17	1970 Aug 12	21 07 55.8	[a]	*OSO 5*	···
18	1970 Oct 26	04 27 06.7	04 31		*SOLRAD 9*
19	1970 Nov 16	14 03 11.7	[b]		[b]
20	1970 Nov 18	03 13 56.0	[b]		[b]
21	1971 Apr 19	18 31 04.4	>18 31 38	*OSO 5*	*SOLRAD 9*
22	1971 Aug 25	16 28 20.0	16 29 12	*OSO 5*	*SOLRAD 9*

[a] No soft X-ray burst detected.
[b] No soft X-ray coverage.

TABLE 2

PARAMETERS DERIVED FROM HARD X-RAY AND SOFT X-RAY OBSERVATIONS

Terms	Definitions
	Hard X-Ray
$S_{28\text{–}254\ \mathrm{keV}}$	Solar flux, 28 to 254 keV, at time of hard X-ray maximum
T_H(HXR peak)	Temperature at time of hard X-ray maximum
ED	Energy density at time of hard X-ray maximum
U	Total thermal energy at time of hard X-ray maximum
	Soft X-Ray
$S_{1\text{–}8\ \text{Å}}$	Solar flux, 1 to 8 Å, at time of soft X-ray maximum
T_S(SXR peak)	Temperature at time of soft X-ray maximum
T_S(HXR peak)	Temperature at time of hard X-ray maximum
EM_S(SXR peak)	Emission measure at time of soft X-ray maximum

ion chamber was determined by calculating the initial current from these data, then translating the current to units of energy per unit time, as follows:

$$F_{\mathrm{OBS}} = (1/eN_{\mathrm{OSO}})\left[(9C_{\mathrm{TOT}}/256+1)\times 10^{R_{\mathrm{TOT}}} - (9C_{\mathrm{BKG}}/256+1)\times 10^{R_{\mathrm{BKG}}}\right] \times 10^{-13}\ \mathrm{ergs\ s^{-1}}, \quad (1)$$

where $1/eN_{\mathrm{OSO}} = 2.23\times 10^8$ ergs coulomb^{-1}; e is the electronic charge in coulombs; N_{OSO}, the number of ion pairs per erg formed in the *OSO 5* ion chamber gas; and R, the range number (0, 1, 2, or 3). In the available *SOLRAD 9* records, the digital output had been deconvolved with the detector response in order to determine the incident solar flux. For purposes of the present work, the energy deposited in that ion chamber was calculated from the reported 1–8 Å solar flux, $f_\odot$, according to the following expression:

$$F_{\mathrm{OBS}} = f_\odot A/QeN_{\mathrm{SOL}} = 1.15\times 10^{-1} f_\odot\ \mathrm{ergs\ s^{-1}}, \quad (2)$$

where A is the detector area in cm^2, Q is the detector-response conversion constant in units of ergs s^{-1} A^{-1}, and N_{SOL} is the number of ion pairs per erg formed in the 1–8 Å *SOLRAD 9* ion chamber gas. N_{SOL} differs slightly from N_{OSO}, due to the difference in atomic composition of the gases in the two ion chambers.

The energy deposited in each of the ion chambers due to emission from the plasma producing the hard X-rays and microwaves at the time of the hard X-ray peak is denoted F_{THERM}. For each burst, F_{THERM} is determined in the following manner: the thermal bremsstrahlung spectrum from a plasma characterized by the temperature and emission measure derived for the hard X-ray/microwave source (see Table 2 of Crannell *et al.* 1978) is calculated; then, this spectrum is convolved with the detector-response function, and the resultant distribution is integrated over energy, effectively $0<E<\infty$. In practice, the integral is performed over the range 0.1 to 1000 keV, which is quite adequate because both of the detector-response functions cut off sharply outside the range 1.5 to 12.4 keV. Because the detector-response function is different for each ion chamber instrument, the value of F_{THERM} for each event is determined independently for the *OSO 5* and *SOLRAD 9* detectors. The following expression provides a quantitative definition of this parameter:

$$F_{THERM} = 1.602\times 10^{-9} A \times \int_{0.1\ \mathrm{keV}}^{1000\ \mathrm{keV}} f_T(E)\cdot \varepsilon(E)\, dE \text{ ergs s}^{-1}, \quad (3)$$

where A is the detector area in cm^2; E denotes photon energy in keV; $f_T(E)$ is the thermal bremsstrahlung spectrum of the burst-related emission; and $\varepsilon(E)$ is the detector-response function. The spectrum defined by $f_T(E)$, in units of ergs cm^{-2} s^{-1} keV^{-1}, depends on the temperature, T, and emission measure, EM, in the following manner:

$$f_T(E) = 2.05\times 10^{-6} EMT^{-0.5} \exp(-E/T) g(E,T), \quad (4)$$

where EM is in units of 10^{45} cm^{-3}; E and T are in keV; and $g(E,T)$ is the temperature-averaged Gaunt factor. The following analytic approximations for $g(E,T)$ were adapted from Tucker (1975), for the designated ranges of E and T:

$$g(E,T) = \begin{cases} (\sqrt{3}/\pi)\ln(2.2T/E) & E<0.36T \\ 1 & 0.36T \le E \le T \\ (T/E)^{0.4} & E>T. \end{cases}$$

The detector-response function, $\varepsilon(E)$, is given by the following expression:

$$\varepsilon(E) = \exp\left[-(M_{W1}X_{W1})-(M_{W2}X_{W2})\cdots-(M_{Wj}X_{Wj})\right] \{1-\exp\left[-(M_{G1}X_{G1})-(M_{G2}X_{G2}) \cdots-(M_{Gk}X_{Gk})\right]\}, \quad (5)$$

where the subscripts $W1, W2, \ldots Wj$ and $G1, G2, \ldots Gk$ denote the atomic constituents of the window and gas portions, respectively, of the ion chamber. The term M_i represents the attenuation coefficient for element i, as a function of energy E, in units of cm^2 g^{-1}; and X_i, the column density of element i in the detector, in units of g cm^{-2}. The attenuation coefficients are obtained from the tables compiled by Veigele (1973), for the energy range 0.1 to 1000 keV. The column densities for the various elements comprising each detector are taken from published and unpublished descriptions of the instruments (Young and Stober 1966; M. P. Nakada, internal GSFC document; D. Horan, private communication; Dere, Horan, and Kreplin 1974). In Table 3, the window and gas components of the ion chambers on *OSO 5* and *SOLRAD 9* are listed together with the corresponding values of the column density.

The temperature and emission measure of the soft X-ray emission at the times of hard X-ray maximum and soft X-ray maximum are derived solely from the *SOLRAD 9* data, using simultaneous measurements of the flux in the 0.5–3 Å and 1–8 Å detectors. The basic technique for determining the temperature from the ratio of the fluxes in the two wavelength bands is described by Dere, Horan, and Kreplin (1974). Subsequent recalibration of the *SOLRAD 9* ion chamber detectors has resulted in an improved set of instrumental parameters for use in temperature and emission measure calculations; these updated parameters were graciously supplied by D. Horan for use in the present work.

The 1 minute temporal resolution of the *SOLRAD 9* instruments necessitated interpolation of consecutive flux measurements to determine the temperature and emission measure at the time of hard X-ray maximum, so these values probably are less reliable than those derived at the time of soft X-ray maximum. The limited dynamic range of the 0.5–3 Å detector also restricts the temperature and emission measure estimates for the two bursts in which the 0.5–3 Å detector became saturated at the soft X-ray peak; for these events, lower limits on the temperature and upper limits on the emission measure were determined. No emission was seen in the 0.5–3 Å detector for two additional events, yielding upper limits on the temperature and lower limits on the emission measure.

For the impulsive emissions, the energy of the source at burst maximum was obtained by Crannell *et al.* (1978)

TABLE 3

CHARACTERISTICS OF THE SOFT X-RAY DETECTORS

Ion Chamber	Detector Area (cm^2)	Elemental Composition	Column Density ($g\ cm^{-2}$) Window[a]	Gas
OSO 5				
(1–8 Å)	1.99	Be	2.34×10^{-2}	...
		Xe	...	1.46×10^{-2}
SOLRAD 9				
(1–8 Å)	1.18	Al	4.10×10^{-5}	...
		Be	2.82×10^{-2}	...
		Ar	3.82×10^{-4}	5.88×10^{-3}
SOLRAD 9				
(0.5–3 Å).....	5.28	Al	4.10×10^{5}	...
		Be	3.14×10^{-1}	...
		Kr	1.61×10^{-3}	2.48×10^{-2}

[a]A layer of gas in the ion chamber which does not contribute to the sensitive volume has the same absorbing effect as additional window thickness.

TABLE 4

CORRELATIONS BETWEEN HARD X-RAY AND SOFT X-RAY PARAMETER PAIRS

Hard X-Ray	Soft X-Ray	r	ν	$P(r,\nu)$
$S_{28-254\ keV}$.....	$S_{1-8\ Å}$	0.114	6	0.807
T_H(HXR peak).....	T_S(SXR peak)	0.041	6	0.931
T_H(HXR peak).....	T_S(HXR peak)	0.422	6	0.345
EM_H(HXR peak) ...	EM_S(SXR peak)	0.285	6	0.536
ED	T_S(HXR peak)	0.309	6	0.501
ED	T_S(SXR peak)	0.071	6	0.879
ED	EM_S(SXR peak)	0.529	6	0.222
U.....	T_S(SXR peak)	0.458	6	0.302
U.....	EM_S(SXR peak)	0.724	6	0.045
U.....	T_S(SXR peak)$\times EM_S$(SXR peak)	0.796	6	0.024

under the assumption of a common thermal source. The parameters employed are the temperature, T, and emission measure, EM, determined from the observed hard X-ray spectrum, and the volume, V, determined from the coincident microwave and hard X-ray observations. The total energy, U, is given by the expression:

$$U=4.8T(V\times EM)^{0.5}, \quad (6)$$

where U is in units of 10^{27} ergs; T in keV; EM in 10^{45} cm^{-3}; and V in 10^{27} cm^3. An alternative expression is:

$$U=4.8TEM/n_e, \quad (7)$$

where n_e is the density in units of 10^9 cm^{-3}.

For the gradual emissions, the soft X-ray observations provide only an effective temperature and emission measure; the actual distributions of temperature and emission measure are not known. Independent observations, required for size or density estimates, are not available. Consequently, the total energy in the soft X-ray source cannot be determined directly. A measure of the energetics is provided by the effective temperature and emission measure, the product of which is approximately proportional to the total energy times the density of the soft X-ray emitting region.

III. ANALYSIS OF RESULTS

The approach adopted in the present work employs direct comparisons of the parameters characterizing each burst to test for possible inconsistencies with thermal models of the impulsive emissions, and to search for fundamental relationships between the gradual and impulsive phenomena. While the results of such analyses should agree, in general, with comparisons of mean characteristics (e.g., Datlowe 1975), correlations or the lack thereof provide considerable additional information regarding causal relationships. The parameter pairs selected to characterize the gradual and impulsive flare emissions are listed in Table 4. Also listed are the

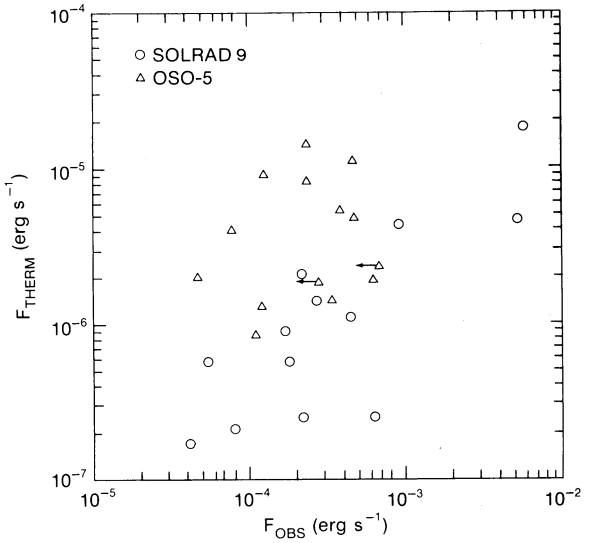

FIG. 2.—Scatter plot of the values of F_{THERM}, the rate of energy deposition expected in the *SOLRAD 9* and *OSO 5* ion chambers based on the temperature and emission measure derived from the hard X-ray observations, vs. the values of F_{OBS}, the rate of energy deposition actually observed.

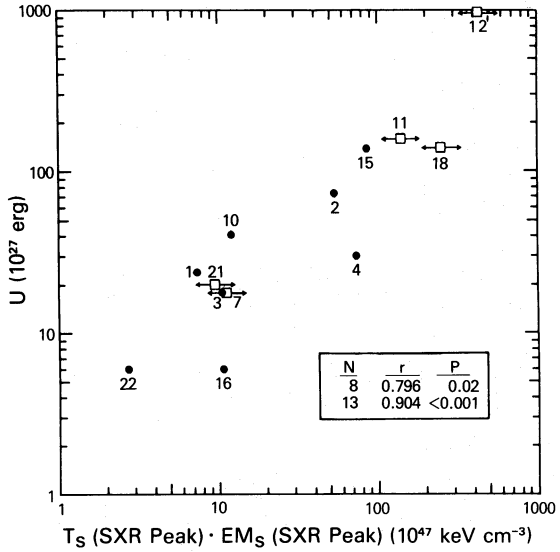

FIG. 3.—Scatter plot of the values of U, the total thermal energy in the hard X-ray/microwave source at the maximum of the impulsive burst, vs. the values of the product T_S(SXR peak)$\times$ EM_S(SXR peak), the temperature and emission measure based on soft X-ray observations at the peak of the soft X-ray emission.

correlation coefficient, r; the number of degrees of freedom, ν; and the probability, $P(r,\nu)$, that a random distribution would show a stronger correlation.

A critical test of any thermal model for the impulsive emissions is a comparison of the energy deposition rate expected in soft X-ray detectors from the postulated thermal bremsstrahlung continuum with the energy deposition rate actually observed. If the observed rate were lower, then models in which the hard X-rays are the result of thermal bremsstrahlung would be definitively ruled out. The values of the expected rate, F_{THERM}, and the observed rate, F_{OBS}, determined as described in the previous section, are shown in Figure 2. From the *OSO 5* soft X-ray data, F_{OBS} is found to satisfy the inequality $10F_{THERM} \leq F_{OBS} \leq 100F_{THERM}$; from the *SOLRAD 9* data, $100F_{THERM} \leq F_{OBS} \leq 1000F_{THERM}$. These results are in agreement with the mean parameters reported by Datlowe (1975) and imply that bremsstrahlung from a hot plasma, of electron temperature and emission measure characterizing the hard X-ray spectrum, provides at most a small fraction of the associated soft X-ray emission. The hypothesis of a thermal origin for the impulsive emissions has not been disproved, therefore, for any of the events investigated.

Each of the parameter pairs listed in Table 4 was tested for evidence of correlation. Of all the pairs tested, only two exhibited significantly positive results:

U with T_S(SXR peak)$\times$ EM_S(SXR peak), and

U with EM_S(SXR peak).

These results are illustrated in Figures 3 and 4, annotated with N, the number of events used in evaluating the correlation ($N=\nu+2$), the correlation coefficient, and the probability. Each of these correlations was evaluated twice, with and without the events for which only limiting values were available.

The lack of correlation between the respective hard X-ray and soft X-ray intensities and emission measures refutes any notion of a direct correspondence between the flare magnitudes in hard and soft X-rays. This is not surprising considering the differences in their time-intensity profiles. It is of particular interest, therefore, that the correlated parameters are those most closely associated with the energetics of the phenomena under consideration: U is the total thermal energy in the hard X-ray and microwave burst source at maximum emission, while T_S(SXR peak)$\times$ EM_S(SXR peak) is approximately the product of the total thermal energy times the density in the soft X-ray emission region. Qualitative and quantitative implications of these results are discussed in detail in the following section.

IV. DISCUSSION AND CONCLUSIONS

The results of this work provide the first direct evidence for a relationship between the energetics of the impulsive and gradual emissions associated with impulsive solar flares. Interpreting the nature of this relationship is complicated because the total energy content, the most explicit measure of the soft X-ray source energetics, is not known. Further progress can be made, never-

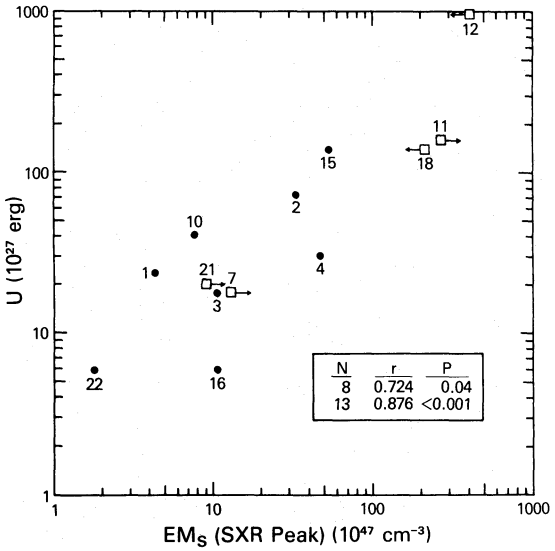

FIG. 4.—Scatter plot of the values of U, the total thermal energy in the hard X-ray/microwave source at the maximum of the impulsive burst, vs. the values of EM_S(SXR peak), the emission measure based on soft X-ray observations at the peak of the soft X-ray emission.

theless, by considering the implications of the observed correlations if the hard X-ray and soft X-ray source regions have the same total energy at their respective maxima. Such an equality is suggested by earlier work based on mean burst parameters (Datlowe, Elcan, and Hudson 1974), and it is supported by the correlations found for the homogeneous set of events analyzed here.

The energy of a thermal source of soft X-rays has the same dependence on temperature, emission measure, and density as does the energy of the corresponding hard X-ray source. If the total peak energy in the soft X-ray source is identical to that of the hard X-ray source, the observed correlation between T_S(SXR peak) $\times EM_S$(SXR peak) and U implies a density in the soft X-ray emitting region of 10^{11} cm^{-3}. This value is consistent with the more recent measurements of Dere *et al.* (1979), Feldman, Doschek, and Kreplin (1980), and others, from spectroscopic observations of density sensitive lines, but it is almost two orders of magnitude greater than typical densities determined for the impulsive source.

The volume of the soft X-ray emitting region, relative to that determined for the hard X-ray spike bursts, also can be inferred from the abovementioned assumption of energy equality and the correlation indicated in Figure 4. These relationships yield a soft X-ray emitting volume which is comparable to but, on average, less than that of the impulsive source. No direct, spatially-resolved observations are available to test this result for the events considered in the present work. Kundu, Alissandrakis, and Kahler (1976), however, have reported similar relationships between relative sizes, based on direct observations with *Skylab* and the NRAO three-element interferometer.

The consistency check reported in § III failed to rule out thermal models for the impulsive emissions. Furthermore, the large quantitive discrepancy between $F_{\rm THERM}$ and $F_{\rm OBS}$, and the disparity between the time scales of the hard and soft X-ray bursts, both imply that the hard X-ray source is not the sole source of the soft X-ray emission. This confirms, for the homogeneous class of simple impulsive events, a conclusion which is widely held for flares in general but which has never been demonstrated heretofore for restricted categories of flare phenomena.

The primary result of the present work is the discovery that the parameters characterizing the energetics of the soft X-ray and hard X-ray emissions are related. This correlation implies that their respective energizing mechanisms are related. The nature of this relationship can be investigated directly with independent measurements of the density and emission measure characterizing the respective source regions. Spectroscopic observations of resolved, density dependent lines now make such determinations possible for the sources of soft X-ray emissions. Spatially resolved observations of hard X-ray and microwave radiation yield equally independent measurements of the volume and emission measure characterizing the sources of these impulsive emissions.

This research was supported in part by NASA grant NSG 033. The authors thank D. M. Horan (NRL) for providing the *SOLRAD 9* observations, as well as the most recent calibration data and the requisite detector parameters. We also thank C. E. Condor and P. J. Kenny (GSFC) for assistance in obtaining and analyzing the *OSO 5* soft X-ray observations. The comments and suggestions of D. M. Horan, C. Hyder, and S. Kahler on this work are gratefully acknowledged.

REFERENCES

Crannell, C. J., Frost, K. J., Matzler, C., Ohki, K., and Saba, J. L. 1978, *Ap. J.*, **223**, 620.
Datlowe, D. W. 1975, in *IAU Symposium 68, Solar Gamma-, X-, and EUV Radiation*, ed. S. R. Kane (Dordrecht: Reidel), p. 191.
Datlowe, D. W., Elcan, M. J., and Hudson, H. S. 1974, *Solar Phys.*, **39**, 155.
Datlowe, D. W., Hudson, H. S., and Peterson, L. E. 1974, *Solar Phys.*, **35**, 193.
de Jager, C. and de Jonge, G. 1978, *Solar Phys.*, **58**, 127.
Dere, K. P., Horan, D. M., and Kreplin, R. W. 1974, *J. Atm. Terr. Phys.*, **36**, 989.
Dere, K. P., Mason, H. E., Widing, K. G., and Bhatia, A. K. 1979, *Ap. J. Suppl.*, **40**, 341.
Elcan, M. J. 1978, *Ap. J. Letters*, **226**, L99.
Feldman, U., Doschek, G. A., and Kreplin, R. W. 1980, *Ap. J.*, **238**, 365.

Kauffman, P., and Iacomo, P., Jr. 1977, "Some Preliminary Results on Time Structures of Solar Microwave Bursts and Apparent Boundary Conditions Regulating the Burst Energy Release with Time" (São Paulo, Brazil: CRAAM/ON/CNPq).
Kreplin, R. W., and Horan, D. M. 1969, NRL Report 6800 (Washington, D.C.: Naval Research Laboratory).
Kundu, M. R., Alissandrakis, C. E., and Kahler, S. W. 1976, *Solar Phys.*, **50**, 429.
Matzler, C., Bai, T., Crannell, C. J., and Frost, K. J. 1978, *Ap. J.*, **223**, 1058.
Neupert, W. M. 1969, *Ann. Rev. Astr. Ap.*, **7**, 121.
Tucker, W. H. 1975, *Radiation Processes in Astrophysics* (Cambridge, Mass.: MIT Press).
van Beek, H. F., de Feiter, L. D., and de Jager, C. 1974, *Space. Res.*, **14**, 447.
_____. 1976, *Space Res.*, **16**, 819.
Veigele, W. J. 1973, *Atomic Data Tables*, **5**, 51.
Wiehl, H. 1976, IAP Report 495 (Berne: University of Berne).
Young, R. M., and Stober, A. K. 1966, NASA TN D-3169.

CAROL JO CRANNELL: Code 684, NASA Goddard Space Flight Center, Greenbelt, MD 20771

JUDITH T. KARPEN: Code 4169K, E.O. Hulburt Center for Space Research, Naval Research Laboratory, Washington, DC 20375

ROGER J. THOMAS: Code 682, NASA Goddard Space Flight Center, Greenbelt, MD 20771